

# Synthesis and Formation of a Supramolecular Nematic Liquid Crystal in Poly(*p*-phenylene–sulfoterephthalamide)–H<sub>2</sub>O

Sebastien Viale,<sup>†,§</sup> Nan Li,<sup>†</sup> Anton H. M. Schotman,<sup>‡</sup> Adam S. Best,<sup>†,§</sup> and Stephen J. Picken<sup>\*,†,§</sup>

Delft University of Technology, Polymer Materials and Engineering, Julianalaan 136, 2628 BL Delft, The Netherlands; Teijin Twaron B.V., Research Institute, P.O. Box 9300, 6800 SB Arnhem, The Netherlands; and Dutch Polymer Institute (DPI), P.O. Box 902, NL-5600 AX, Eindhoven, The Netherlands

Received November 25, 2004; Revised Manuscript Received February 10, 2005

**ABSTRACT:** The formation of lyotropic solutions in water has yet to be reported for polyaramides. In this work, we investigate the synthesis and properties of a water-soluble polyaramid via the inclusion of a sulfonated monomer in the backbone of the polymer chain. Using sulfonated terephthalic acid (sTA) together with a diamine and a diisocyanate enables us to produce a lyotropic water-soluble polyaramid poly(*p*-phenylene–sulfoterephthalamide). Two different synthetic routes are presented: (1) the reaction between sTA and *p*-phenylene diisocyanate (PPDI) and (2) the reaction of activated sTA using triphenyl phosphite and *p*-phenylenediamine (PPD). Polymers with various molar masses up to 15 000 g mol<sup>-1</sup> using both methods have been obtained. We have examined the optimal reaction conditions for the synthesis of these polymers, in particular the effect of reaction temperature, concentration of monomers and reactants, type of counterions, and solvents. The polymers obtained are mostly soluble in water, up to high concentration (10 wt % without an alkali counterion on the sulfonic acid group), and surprisingly lyotropic nematic behavior has been observed independent of the molar mass of the polymer. The phase diagram of these materials in water has been investigated, and the lyotropic phase has been characterized using optical polarized microscopy.

## Introduction

The enhancement in solubility of polyaramides has been an important area of research in the past few years. To reveal the liquid crystalline properties of polyaramides such as Kevlar and Twaron, sulfuric acid is the solvent of choice. This is due to the hydrophobic nature of the aromatic backbone in combination with strong intermolecular hydrogen bonding between the chains that reduces the solubility of polymer and leads to a high melting point.<sup>1</sup> Several papers have reported structural modifications of PPTA via three main strategies: (1) disturbing the stiffness of the polymer chains, (2) increasing the distance between the polymer chains, and (3) improving the solubility of the polymer backbone in water through the introduction of ionizable moieties.

By introducing defects along the polymer chains, such as kinked and double kinked monomers and nonplanar monomers, Preston et al.<sup>2–4</sup> reduced the chain stiffness, but also the lyotropic behavior was lost. These modifications improved the solubility in aprotic polar amide solvents such as dimethylacetamide (DMAc) or *N*-methylpyrrolidone (NMP) after the addition of salt (CaCl<sub>2</sub> and LiCl). However, it appears that this approach is not successful in terms of formation of a liquid crystalline phase in organic solvents; solubility is improved at the expense of the lyotropic liquid crystal formation.

Increasing the distance between the polymer chains may reduce the formation of hydrogen bonds and increase the solubility while preserving the lyotropic

behavior. In this approach the polymer backbone stiffness is not disturbed. The bulky substituents used by Kricheldorf et al.,<sup>5–8</sup> such as aromatic rings, have been shown to increase the solubility of the final materials, but no clear liquid crystalline behavior has been obtained in solution.

In a recent paper,<sup>9</sup> we reported on the upgraded synthesis of a sulfonated water-soluble PPTA, poly(*p*-sulfophenylene–terephthalamide), **P1**, previously described by Vandenberg et al.<sup>10</sup> Unfortunately, again no clear liquid crystalline phase was observed due to gel formation. Small-angle neutron experiments revealed the formation of molecular aggregates upon increasing counterion concentration in solution.<sup>11</sup> Similar results have been reported by Chu et al.<sup>12,13</sup>

In a recent communication,<sup>14</sup> we presented some preliminary results on the synthesis and the solution properties of a novel polymer, poly(*p*-phenylene–sulfoterephthalamide or “Sulfo Invert PPTA”): **P2** (see Figure 1). In the present paper, we will present the polymerization conditions using two different, but well-known, synthetic routes (see Figure 2): (1) a diisocyanate route<sup>15–19</sup> and (2) a direct phosphorylation route.<sup>20–22</sup> We will also discuss the critical role played by the sulfonic acid group on the gel formation of **P1** observed by others and ourselves. The observation of a free-flowing supramolecular lyotropic nematic phase in **P2** provides some insight into the underlying mechanism for the gel formation in **P1**. The phase diagram and the liquid crystalline behavior of **P2** will be thoroughly investigated in this work.

## Experimental Section

**General Methods.** <sup>1</sup>H and <sup>13</sup>C NMR were recorded in D<sub>2</sub>O and DMSO-*d*<sub>6</sub> on a 300 MHz UR-300S Varian. Size exclusion chromatography (SEC) was performed by dissolving the

<sup>†</sup> Delft University of Technology.

<sup>‡</sup> Teijin Twaron B.V., Research Institute.

<sup>§</sup> Dutch Polymer Institute.

\* Corresponding author: Fax +31 15 2787415; e-mail s.j.picken@tnw.tudelft.nl.

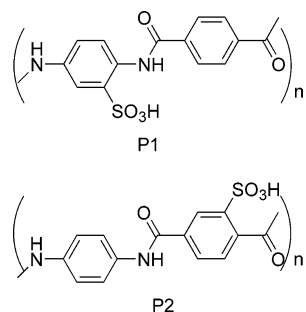


**Figure 1.** Structures of Sulfo PPTA, **P1** (top), vs Sulfo Invert PPTA, **P2** (bottom).

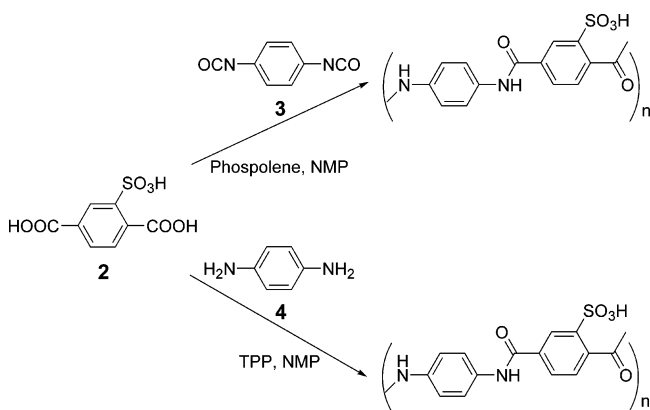


**Figure 2.** Polymerization routes investigated in this study: top, diisocyanate route; bottom, phosphorylation route.

polymeric sample in concentrated sulfuric acid (1 mg/mL) and separating this using a modified Zorbax column (250 × 6.2 mm) and concentrated sulfuric acid as the mobile phase (0.1 mL/min). A UV detector operating at 340 nm was used. From the chromatograms, the molar mass values were calculated using Cirrus version 1.1 GPC software (Polymer Labs). As standard references for the SEC analysis, a Twaron (PpPTA) yarn type 1010 (the molar mass which has been previously determined by DLS as 30 000 g mol<sup>-1</sup>) and an Aramid trimer were used. The salt content in our polymers was determined by flame atomic absorbance spectroscopy (FAAS) using a Perkin-Elmer Plasma 40 flame atomic absorbance spectrometer. To characterize the phase behavior in aqueous solution, the polymer samples were dissolved in hot water using ultrasonic mixing at 60 °C for 2 h prior to analysis. Thermogravimetric analysis (TGA) measurements were performed on the solid polymer samples in the form of a powder using a Perkin-Elmer TGA 7a, with the sample under a flow of nitrogen and with a heating rate of 10 °C/min from 25 to 400 °C.

**Materials.** *N*-Methylpyrrolidone (99.99% Aldrich Sure Seal), dimethylacetamide (99.99% Aldrich Sure Seal), triphenyl phosphite (99%+, Aldrich), and pyridine (99.99% Aldrich Sure Seal) were used as received. 2,5-Dimethylbenzenesulfonic acid (**1**, Acros 99%), 1,4-phenylene diisocyanate (**3**, Aldrich 99%), 1,4-phenylenediamine (**4**, 99% provided by Teijin Twaron), and 3-methyl-1-phenyl-2-phospholene 1-oxide (**5**, ABCR, 99%) were used as received. Dowex-50wx4-200, (Sigma-Aldrich), lithium chloride (Aldrich, 99+%), and calcium chloride were dried under vacuum in an oven at 250 °C overnight. Other solvents are of technical grade.

**2-Sulfoterephthalic Acid (2).** In a 1 L reactor vessel equipped with a mechanical stirrer and a cooler, 20.84 g (0.111 mol) of **1** was dissolved in 500 mL of water, and then 82.36 g (0.52 mol) of KMnO<sub>4</sub> was added stepwise for 5 h. The reaction mixture was heated at reflux for 48 h, followed by filtering to remove the residual MnO<sub>2</sub>. The filtrate was ion exchanged with Dowex (three times) to remove the K<sup>+</sup> from the sulfonic acid group. HCl was then added to the filtrate, and immediate precipitation of **2** occurred. The yield was 15 g (54.5%). <sup>1</sup>H NMR

(DMSO-*d*<sub>6</sub>): δ 8.33 (s, 1H), 8 (dd, 1H, *J* = 1.8 Hz, *J* = 8.1 Hz), 7.69 (d, 1H, *J* = 7.8 Hz). <sup>13</sup>C NMR (DMSO-*d*<sub>6</sub>): δ 169, 167 (COOH), 145, 136.1, 132.6, 130.7, 130.3, 128.6.

**Polymerization.** The polymerization and all transfer operations were carried out in flame-dried glassware and under argon due to the high moisture sensitivity of the reactants. After assembly, the equipment was heated and flushed with argon to remove any absorbed moisture. During the reaction, argon was slowly flushed through the reactor. The reactor consists of a 250 mL three-necked flask, equipped with a cooler, argon inlet and outlet, and a thermometer. The reactor was heated with a thermo-regulated oil bath. Because of the batch sizes used in this work, a magnetic stirrer was used during the polymerization. A mechanical stirrer was considered to be inappropriate for the present batch size; however, the use of such a device is acknowledged to assist in obtaining higher molar mass in analogous pPPTA polymerization reactions.

**Diisocyanate Route, Optimum Conditions.** 1.74 g (10.09 mmol) of **3** and 3.9 g (20.31 mmol) of phospholene catalyst **5** were dissolved in NMP with 2.63 g of LiCl. The solution was heated at 75 °C for 1 h, and then 2.67 g (10.09 mmol) of **2** dissolved in NMP was added. The reaction mixture is heated at 115 °C for 3 h. The yellow viscous solution was precipitated in 400 mL of methanol. A yellow precipitate was obtained which was filtered and washed with methanol (500 mL) and with diethyl ether (500 mL). The goldish powder is dried under vacuum at 80 °C overnight. The yield was 4 g (91%). <sup>1</sup>H NMR (DMSO-*d*<sub>6</sub>): δ 11.5 ppm (1H, s, NHCO), 10.5 ppm (1H, s, NHCO), 9.9 ppm (t, *J* = 7.8 Hz, 2H), 8.6 ppm (t, *J* = 7.8 Hz, 2H), 8.1 ppm (t, *J* = 8.1 Hz, 3H). <sup>13</sup>C NMR (DMSO-*d*<sub>6</sub>): 164 ppm, 162 ppm C=O, δ 145.2, 142.8, 138.3, 135.8, 129.7, 129.2, 128.2, 127.8, 127.6, 127.4, 127.1, 126.8.

**Phosphorylation Route, Typical Procedure.** 1 g (4.06 mmol) of **2**, 2.90 g (9.34 mmol) of TPP, 3.28 g of LiCl, and 8.20 mL of pyridine were dissolved in 40 mL of NMP. The solution was heated 40 °C for 15 min, and then 0.76 g (4.06 mmol) of **4** was added. The reaction mixture was heated at 115 °C for 4 h. The yellow viscous solution was precipitated in 500 mL of methanol. A yellow precipitate was obtained. The precipitate was filtered and washed with methanol (500 mL) and diethyl ether (500 mL). The gold-colored powder was dried under vacuum at 80 °C overnight; the yield was 1.1 g (77%). <sup>1</sup>H NMR (DMSO-*d*<sub>6</sub>): δ 11.32 ppm (1H, s, NHCO), 10.5 ppm (1H, s, NHCO), 8.85 ppm (s, 1H), 8.48 ppm (s, 1H), 7.5 ppm (q, 4H), 7.34 ppm (s, 1H). <sup>13</sup>C NMR (DMSO-*d*<sub>6</sub>): 165.26 ppm, 164.37 ppm C=O, δ 144.4, 143.6, 130.7, 129.4, 128.3, 126.5, 125.9, 125.7, 120.9, 120.7, 120, 119.9.

## Results and Discussion

**1. Diisocyanate Route.** To determine the effect of all the parameters examined in this study, SEC analysis has been used to obtain a crude estimation of the molar mass of the polymers prepared. Diisocyanate monomers together with sTA, **2**, produce polyaramides with the aid of a phospholene catalyst. The catalyst requires time to react with the diisocyanates in order to form carbodiimides prior to the polymerization reaction.<sup>16</sup> To achieve this the monomer should be activated first at a certain temperature and for a certain time. To determine the optimal reaction conditions, different reaction times have been studied, namely, no activation of the monomers, 1 h, 2 h, and 3 h of activation. Our experimental results show that the best conditions are 1 h at 75 °C.

An important issue is the choice of the solvent as the reaction medium. It has been already reported that carbodiimides can react with NMP and DMAc.<sup>19</sup> To reduce this side reaction the best solvent is sulfolane, however, our monomers are insoluble in sulfolane, and therefore, we decided to use NMP instead. To reduce the possible side reaction between the carbodiimide and

the solvent, we carefully tuned the monomer concentration and found that (10 mmol) was the best concentration to prevent side reactions that can alter the final molar mass.

Under these carefully chosen conditions, the carbo-diimides can react further with the sulfonated terephthalic acid. We investigated the time and temperature dependence of the polymerization reaction. The effect of temperature on the final molar mass has been studied, with three different temperatures were used: 75, 115, and 125 °C. The highest molar mass obtained for the final polymer was at 115 °C.

The effect of reaction time on the reaction has been followed by SEC and NMR. 2 mL of the reaction mixture was extracted every 1 h and precipitated in methanol and washed. These samples have been analyzed using SEC, and the results clearly show that the reaction takes place rapidly and the molar mass reaches a plateau value of 8000 g mol<sup>-1</sup> after 3 h of reaction. We found that 115 °C combined with 3 h of reaction time produces the highest molar mass polymer with this method. Using this optimized diisocyanate route, polymers of **P2** with reasonable molar masses were obtained of between 8500 and 13 000 g mol<sup>-1</sup>. A further increase of the molar mass would be anticipated on increasing the batch size.

The solubility problem of polyaramides has been previously discussed by Otsuki,<sup>21</sup> and it has been shown to have a dramatic effect on the final molar mass of this class of polymer.<sup>22</sup> The use of symmetric monomers may also affect the final molar mass of the polymer due to the formation of a linear polyaramide that can precipitate during the polymerization, thereby reducing the final molar mass.<sup>19</sup> Consequently, the amount of NMP used at the early stage of the polymerization has to be tuned carefully in order to prevent undesired precipitation. A high-shear mechanical stirring device, to prevent the precipitation of the polymer, and a larger batch size can be used to increase the final molar mass.

**2. Phosphorylation Route.** The more classical synthesis route is via the use of a phosphorylation method,<sup>20–22</sup> and this has also enabled us to produce high molar mass polymers of **P2**. To obtain the optimum reaction parameters, again a number of conditions have been carefully investigated.

Our first concern was the reaction temperature, as already reported in the literature<sup>23</sup> this has been found to play a major role in the final molar mass of aramid-based polymers. Different temperatures have been studied: 75, 115, and 125 °C, with the highest molar mass polymers obtained at 115 °C.

The reaction time has also been studied using offline SEC to determine the kinetics of the reaction. To achieve this, 2 mL of the reaction mixture was extracted every hour and precipitated in methanol and washed. After 4 h, the molar mass was found to reach a maximum, and no further increase was observed.

Monomer concentration as well as the monomer feed has been investigated. As observed in industrial processes, the impact of monomer concentration and monomer feed is crucial. We observe a tremendous increase in the molar mass when the monomer concentration is high (3.3 mol) and the monomer feed is continuous (total 10 g). No effect on the final molar mass of the polymer was observed with different choices of salt, namely LiCl and CaCl<sub>2</sub>, solvent (NMP or DMAc), and the rate of addition of the monomers.

**Table 1. Solution Behavior of the Polymers Obtained in This Study**

molar mass	[Li], wt %	water solubility <sup>a</sup>	LC <sup>b</sup>
1400	0.01 <sup>c</sup>	+	no
1900	0.01 <sup>c</sup>	+	no
1800	1.12	+	no
1700	1.01	+	no
1300	0.34	+++	yes
1500	0.64	+++	yes
1600	0.30	+++	yes
1800	0.36	+++	yes
1900	0.30	+++	yes
2000	0.40	+++	yes
2700	0.64	+++	yes
8500	0.43	+++	yes
6000	0.40	+++	yes
13000	0.30	+++	yes
15000	0.42	+++	yes

<sup>a</sup> Polymer powder dissolved in water and boiled for 15 min. <sup>b</sup> LC = liquid crystalline behavior, observation based on 6 wt % solution. <sup>c</sup> Synthesis with CaCl<sub>2</sub>; +, inhomogeneous solution; +++, clear yellow solution.

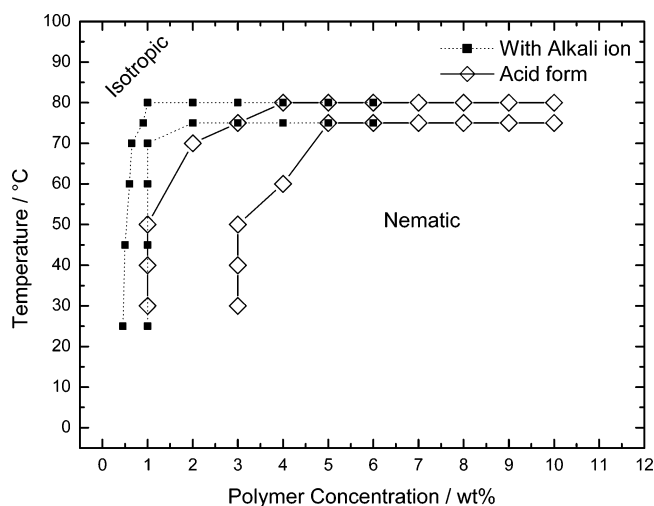


**Figure 3.** Phase diagram of **P2** as a function of temperature and polymer concentration, with alkali ion (■) and acid form (◇).

**3. Phase Diagram.** As mentioned previously in the Introduction, no clear lyotropic behavior was observed for **P1** in water due to the formation of a gel phase. We have briefly described the polymer **P2**, as obtained via the phosphorylation or the diisocyanate route, is soluble in water and can show liquid crystalline behavior at rather low polymer concentration. In Table 1 some solubility results are summarized where the LC behavior is evaluated at 6 wt % polymer concentration.<sup>14</sup>

For solutions of **P1**, when the alkali ion concentration is high (5 wt %), the polymer is not soluble in water and no liquid crystalline behavior is observed. This behavior has been attributed<sup>19</sup> to the hydrogen-bonding interactions between the sulfonic acid group and the water, which are screened due to the presence of the alkali metal ion, resulting in a behavior similar to that of PPTA in water.

Figure 3 shows the phase diagram of Sulfo invert PPTA with two different samples: in the presence of alkali ion and in the acid form. With alkali ion (K<sup>+</sup>, 3.3 wt %) as the counterion, 6 wt % represents the solubility limit of the polymer; at higher polymer concentrations the powder absorbs the water and swells. Interestingly for the samples in the acid form, the solubility limit is increased to 10 wt %. This observation can be explained by the alkali ion inducing greater aggregation of the

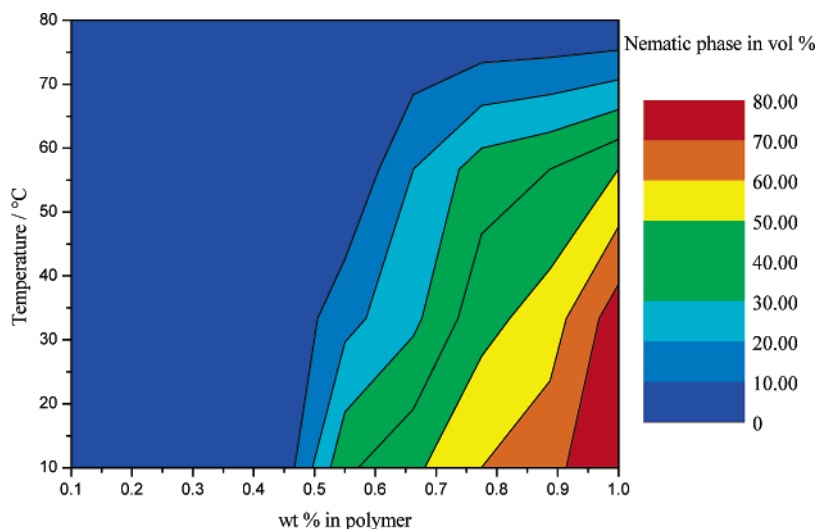


**Figure 4.** Evolution of the fraction of the isotropic phase in the biphasic region as a function of temperature.

polymer chains, and therefore the sizes of the aggregates in solution are bigger. Consequently, the solubility limit is higher for the sample without any alkali ions due to the smaller size of the aggregates, which delays precipitation.

The phase behavior shown in Figure 3 appears to consist of two different phase diagrams superimposed on each other; at low temperature between 10 and 70 °C a more or less athermal biphasic region can be observed which can be modeled using excluded volume based theories like Onsager or Khokhlov–Semenov theory, while the upper limit (70–80 °C) of the nematic phase seems to be related to the stability of the supramolecular assemblies themselves, i.e., it represents a transition from a supramolecular to a molecular solution. Some preliminary results from XRD indicate that below 0.5 wt % a transition from a supramolecular to molecular structure can be observed at approximately 70–80 °C.<sup>14</sup>

To explore the biphasic region of the solutions with potassium as the counterion in more detail, 10 samples between 0.1 and 1 wt % polymer have been prepared, and the results are shown in Figure 4.

For both systems, with and without potassium counterions, the biphasic region is only slightly affected by the temperature, revealing that we are dealing with an athermal liquid crystal phase. The upper limit between N → I, at approximately 70–75 °C for both samples, is due to the destruction of the aggregates, which form the building blocks of the nematic phase.

From the phase diagram, we conclude that the supramolecular aggregates behave like an athermal liquid crystal where the formation of the LC phase is mainly governed by the excluded volume interaction of the aggregates. When the temperature is increased, the aggregates disappear, resulting in a molecular solution. At these elevated temperatures the molecular solution should become liquid crystalline at higher polymer concentrations, but we did not succeed in observing this due to the evaporation of the solvent which resulted in inhomogeneous samples.

**4. Optical Polarized Microscopy (OPM).** Considering the wide range of molar masses of polymers explored in this work, we can clearly show that the formation of LC phase is independent of molar mass and, to a lesser degree, salt concentration. In all cases, molecular aggregates are formed and become aligned

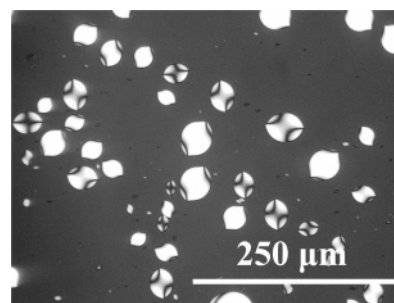


**Figure 5.** Biphasic solution of sample 190 at 0.5 wt % in water (magnification 300×).

to form a nematic solution; this result has been confirmed in a recent publication.<sup>14</sup>

Isotropic solutions are observed for low polymer concentrations in the presence of K<sup>+</sup>, up to 0.5 wt % polymer in water and up to 1 wt % in the acid form. A biphasic system is observed in both cases using optical polarization microscopy. Nematic droplets with characteristic Maltese crosses are dispersed in surrounding isotropic solution, as shown in Figure 5.

Upon increasing the polymer concentration, the isotropic phase disappears. A homogeneous nematic phase is obtained at a concentration of 2–6 wt % in the presence of alkali ions, and the samples show a characteristic Schlieren texture. In the case of the acid form, the phase boundary is shifted to 3 wt %, and similar textures are observed.

It is remarkable to note that the nematic solution is obtained for a relatively low weight fraction of polymer, and the birefringence of these solutions is relatively high, implying the molecules are highly oriented. For these concentrations, colored nematic textures are obtained, as shown in Figure 6.

**5. Gel Formation.** The striking result of this work is the lack of gel formation in solution when compared to **P1**. Further investigation has been done in order to understand the difference in the solution behavior of the two polymers. As a first approximation, we can establish the following: the structures of **P1** and **P2** differ only by the distance between the sulfonic acid group and the neighboring amide group, and therefore **P2** is more soluble in water than **P1**.<sup>24</sup>

The probable cause for the decrease in the solubility of **P1** is the formation of an intramolecular hydrogen

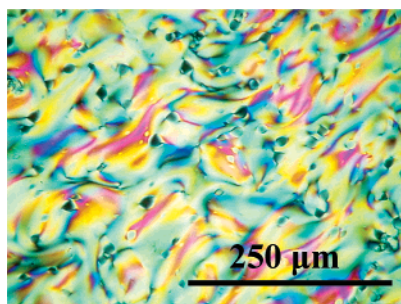


**Figure 6.** Nematic solution of containing alkali ions (molar mass  $2000 \text{ g mol}^{-1}$ ) at 6 wt % in water (magnification  $300\times$ ).

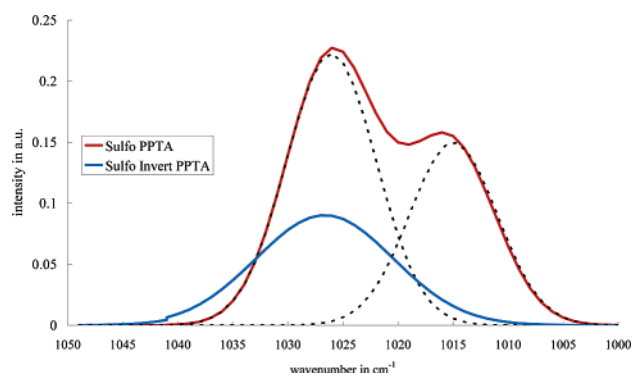


**Figure 7.** FTIR of the sulfonic acid group on **P1** (red) and **P2** (blue) in solution (5 wt % in water).

bond between the sulfonic acid group and the hydrogen from the amide bond. Therefore, the sulfonic acid group is not fully involved in hydrogen bonding with the water, which reduces the solubility of the polymer backbone and enhances gel formation. Figure 7 confirms this hypothesis, as the FTIR spectra of the region of  $\nu_s(\text{SO}_3)$  vibration from  $1050$  to  $1000 \text{ cm}^{-1}$  of sulfonic acid group shows a shoulder for **P1**; this corresponds to a change in the polarizability of the bond due to the interaction with hydrogen of the neighboring amide bond.<sup>25,26</sup> A similar observation of hydrogen bonding between a sulfonic acid group and water has been reported for Nafion.<sup>27</sup> It is not possible to check the character of the amide vibration, as this is obscured by the O–H stretch of water ( $3200 \text{ cm}^{-1}$ ).

Finally, if an additional hydrogen bond is formed between the sulfonic acid group and the hydrogen of the amide bond, it is expected that the thermal stability of the sulfonic acid group should increase. This is confirmed by TGA measurement performed on samples with similar molar mass and counterion concentrations, and the curves are shown in Figure 8.

A noticeable drop in mass is observed for **P2** around  $220$ – $280 \text{ }^\circ\text{C}$  due to the departure of the sulfonic acid group<sup>9</sup> (blue curve).<sup>19</sup> This is less pronounced in the case of **P1** (red curve).<sup>28</sup>

Because of the larger distance between the hydrogen of the amide bond and the sulfonic acid group in **P2**, no intramolecular hydrogen bond is formed; therefore, the sulfonic acid group can fully play its role as an ionizable group, and this enhances the water solubility of the polymer backbone. This effect will be examined further in an upcoming publication using computational modeling.<sup>29</sup>

## Conclusions

Synthesis of a new water-soluble synthetic lyotropic polymer, “Sulfo Invert PPTA”, is reported. Two different

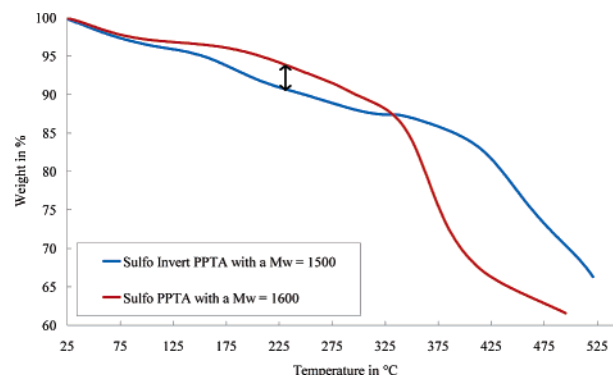


**Figure 8.** TGA of **P2** and **P1**. Note the drop in mass at  $225 \text{ }^\circ\text{C}$  in the case of Sulfo Invert PPTA.

synthetic routes have been pursued: a diisocyanate-based route and the activation of the monomers using phosphorylation. Reasonably high molar masses are obtained, corresponding to a degree of polymerization of about 30, for both routes.

Importantly, liquid crystalline behavior in water has been observed and characterized for a modified PPTA. It appears that this is due to the presence of supramolecular aggregates in the solution, and this is confirmed by the characteristic athermal lyotropic behavior for the transition from the isotropic to the nematic phase.

In a molecular liquid crystal system, the concentration for the I–N transition would be expected around 12 wt %, whereas in our system the formation of a nematic phase occurs at very low concentration (below 1 wt %), characteristic of a supramolecular liquid crystal phase. The effect of the salt on the phase diagram has been also determined, where the critical concentration increases when the sample contains no salt.

Finally, no gel formation was observed in Sulfo Invert PPTA, which is attributed to the lack of intramolecular hydrogen bonding between the amide and sulfonic acid group, enhancing the solubility of the final polymer. A forthcoming paper will discuss the solution behavior of the supramolecular aggregates using X-ray and SANS experiments.

**Acknowledgment.** We thank Dr. E. Mendes for discussions on the structure of the supramolecular solutions. This work forms part of the research program of the Dutch Polymer Institute.

## References and Notes

- (1) Kwolek, S. L.; Morgan, P. W.; Schaeffgen, J. R.; Gulrich, L. W. *Macromolecules* **1977**, *10*, 1390.
- (2) Preston, J. *Polym. Eng. Sci.* **1975**, *15*, 199.
- (3) Preston, J.; Smith, R. W.; Sun, S. M. *J. Appl. Polym. Sci.* **1972**, *16*, 3237.
- (4) Gaudiana, R. A.; Minns, R. A.; Rogers, H. G.; Kalyanaraman, C.; McGowan Hollinsed, W. C.; Manello, J. S.; Sahatjian, R. *Macromolecules* **1985**, *18*, 1085.
- (5) Kricheldorf, H. R.; Schmidt, B.; Birger, R. *Macromolecules* **1992**, *25*, 5465.
- (6) Kricheldorf, H. R.; Schmidt, B. *Macromolecules* **1992**, *25*, 5471.
- (7) Kricheldorf, H. R.; Schmidt, B. *Macromolecules* **1992**, *25*, 6090.
- (8) Kricheldorf, H. R.; Domschke, A. *Macromolecules* **1994**, *27*, 1506.
- (9) Viale, S.; Jager, W. F.; Picken, S. J. *Polymer* **2003**, *44*, 7843.
- (10) Vandenberg, E. J.; Diveley, W. R.; Filar, L. J.; Patel, S. R.; Barth, H. G. *Polym. Prepr.* **1988**, 139.
- (11) Mendes, E.; Viale, S.; Santin, O.; Heinrich, M.; Picken, S. J. *J. Appl. Crystallogr.* **2003**, *36*, 1000.

- (12) Chu, E. Y.; Xu, Z. S.; Lee, C. M.; Sek, C. F. K.; Okamoto, Y.; Pearce, E. M.; Kwei, T. K. *J. Polym. Sci., Part B: Polym. Phys.* **1995**, *33*, 71.
- (13) Yun, H. C.; Chu, E. Y.; Han, Y. K.; Lee, J. L.; Kwei, T. K.; Okamoto, Y. *Macromolecules* **1997**, *30*, 2185.
- (14) Viale, S.; Best, A. S.; Mendes, E.; Jager, W. F.; Picken, S. J. *Chem Commun.* **2004**, 1596.
- (15) Otsuki, T.; Kakimoto, M. A.; Imai, Y. *J. Polym. Sci., Part A: Polym. Chem.* **1989**, *27*, 1775.
- (16) Otsuki, T.; Kakimoto, M. A.; Imai, Y. *J. Polym. Sci., Part A: Polym. Chem.* **1988**, *26*, 2263.
- (17) Simionescu, C.; Comanaita, E.; Vata, M. *Angew. Makromol. Chem.* **1975**, *46*, 135.
- (18) Simionescu, C.; Comanaita, E.; Vata, M. *Angew. Makromol. Chem.* **1976**, *50*, 15.
- (19) Schotman, A. H. M.; Weber, T. J.; Mijs, W. J. *Macromol. Chem. Phys.* **1999**, *200*, 635.
- (20) Yamazaki, N.; Mastumoro, N.; Higashi, F. *J. Polym. Sci., Part A: Polym. Chem.* **1975**, *13*, 1373.
- (21) Higashi, F.; Ogata, S.-I.; Aoki, Y. *J. Polym. Sci., Part A: Polym. Chem.* **1982**, *20*, 2081.
- (22) Krigbaum, W. R.; Kotek, R.; Mihara, Y.; Preston, J. *J. Polym. Sci., Part A: Polym. Chem.* **1984**, *22*, 4045.
- (23) Russo, S.; Mariani, A.; Mazzani, S. L. E. *Macromol. Symp.* **1997**, *118*, 73.
- (24) The structures of **P1** and **P2** (similar molar mass) have been carefully checked by NMR and are in accordance with the hypothesis.
- (25) Böhner, U.; Zundel, G. *J. Phys. Chem.* **1985**, *89*, 1405.
- (26) Langner, R.; Zundel, G. *J. Phys. Chem.* **1995**, *99*, 12214.
- (27) Ludvigsson, M.; Lindgren, J.; Tegenfeldt, J. *Electrochim. Acta* **2000**, *45*, 2267.
- (28) Further investigations have been done using XRF in order to determine the content of sulfur in the sample before and after exposure at 280 °C. We found for starting polymers: 8.0% in mass of sulfur (calculated 10.04%), after exposure 0.1% in mass of sulfur (calculated 0%). The loss weight difference is 10% at 225 °C.
- (29) Grozema, F. C.; Best, A. S.; van Eijk, L.; Stride, J.; Kearley, G. J.; de Leeuw, S. W.; Picken, S. J. *J. Phys. Chem. B*, in press.

MA0475636